

A real-time prediction method of slope failure using Bayesian approach based on slope surface tilting measurements[☆]

Nuo Chen ^{a,b}, Pengpeng He ^c, Jiaxun Chen ^a, Xiaocheng Huang ^d, Kun Fang ^e, Jiren Xie ^{a,*}, Denis N. Gorobtsov ^f, Margarita A. Novgorodova ^f

^a Department of Civil Engineering, Central South University, Changsha 410075, Hunan Province, China

^b Department of Civil Engineering, The University of Hong Kong, Central and Western District, 999077, Hong Kong, China

^c School of Science and Engineering, University of Dundee, Dundee DD1 4HN, UK

^d School of Civil Engineering, Hunan University of Science and Technology, Xiangtan, Hunan Province 411100, China

^e Department of Civil Engineering and Environmental Engineering, The Hong Kong University of Science and Technology, Kowloon 999077, Hong Kong, China

^f Sergei Ordzhonikidze Russian State University for Geological Prospecting, Miklouho-Maclay St. 23, Moscow 117997, Russian Federation

ARTICLE INFO

Keywords:

Tilting
Slope failure time
Bayesian method
Landslides

ABSTRACT

In recent years, slope failure prediction methods using surface tilting measurements have been developed and applied to landslide mitigation. However, it is still challenging to obtain the exact slope failure time because of the uncertainties in monitoring data. Existing methods are unable to provide a failure time interval with a defined confidence level, which is crucial for reliable field predictions by governments and researchers. In this paper, a novel landslide prediction method using the Bayesian approach and based on surface tilting measurements was proposed to estimate an accurate interval of slope failure time, which also allows dynamic updates as new monitoring data become available. Tests at different scales have been used to validate this method. Additionally, A comparison with the conventional prediction method indicates that the proposed prediction method provides more robust and accuracy failure time estimations. Furthermore, the relationship between prediction errors and input data quantity was also investigated using fifteen laboratory and field test cases. Regressive formulas with 95 % confidence were obtained, which provides a valuable guidance for estimating prediction errors based on data availability in practice.

1. Introduction

Landslides typically refer to sudden and devastating rock or soil slope collapse resulted from the interaction of geological conditions and meteorological phenomena, such as rainfall. This disaster poses substantial threats to communities, infrastructure, and natural ecosystems, causing severe economic losses and a large number of casualties in mountain regions every year (Petley, 2012; Klose et al., 2016; Hu et al., 2021; Satgada et al., 2023; Gong et al., 2024; Bruland et al., 2025). To mitigate landslide-induced damage, traditional solutions including retaining walls and anchors are often used to improve slope safety factors. However, high economic cost, long time of construction, and complicated site conditions limit their wide applications, especially in low-income countries and regions. (Uchimura et al., 2015; Smethurst

et al., 2017; Dixon et al., 2018; Al-Jawadi et al., 2021). In recent years, advances in remote sensing technology and Internet of Things (IoT) have led to the development of different prediction methods using surface displacement monitoring, which has been recognized as promising approaches to mitigate landslide damages (Saito, 1969; Fukuzono, 1985; Voight, 1988; Teuku et al., 2016; Smethurst et al., 2017; Wang et al., 2022a, 2022b; Al-Jawadi, 2024; Cui et al., 2024; Fang et al., 2025; Zhou et al., 2025). Typical landslide prediction methods, such as the Materials Failure Forecasting Method (FFM), were normally derived from slope displacements, and have been adopted as a crucial methodology in landslide prediction (e.g., Saito, 1965; Fukuzono, 1985; Voight, 1988; Petley et al., 2005; Mufundirwa et al., 2010; Stähli et al., 2015; Hao et al., 2016; Zeng et al., 2024). Although the FFM has been validated by a variety of landslide events, the complexity in instrument installation

[☆] This article is part of a Special issue entitled: 'Landslides Prediction' published in Engineering Geology.

* Corresponding author.

E-mail addresses: nuochen011102@connect.hku.hk (N. Chen), phe001@dundee.ac.uk (P. He), kunfang@cug.edu.cn (K. Fang), jirenxe198911@csu.edu.cn (J. Xie), gorobtsovndn@mri.ru (D.N. Gorobtsov), novgorodovama@mri.ru (M.A. Novgorodova).

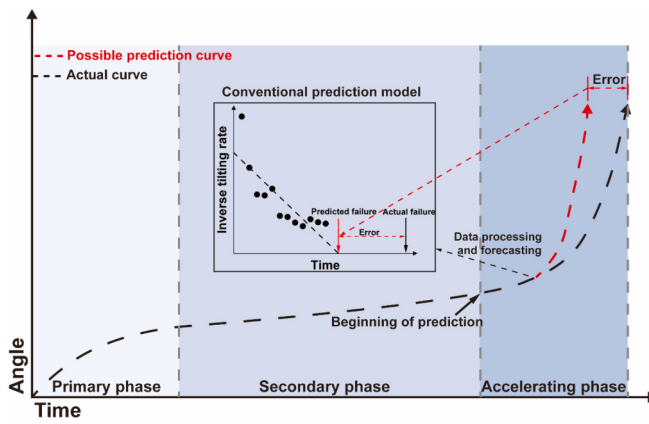


Fig. 1. Creep curve and error of slope failure prediction by tilting prediction model.

and maintenance restricts its application (Uchimura et al., 2015; Xie et al., 2020). While InSAR and LiDAR can partially address these limitations (Wasowski and Bovenga, 2014; Wasowski and Pisano, 2019; Sun et al., 2021; Pang et al., 2023; Fan et al., 2024; Lv et al., 2025), their relatively low resolution and monitoring frequency still limit their application in landslide detection (Xie et al., 2020).

Recently, a new slope monitoring technique based on MEMS (Micro Electro Mechanical Systems) was proposed, with lower costs and simpler installation (e.g., Towhata et al., 2005; Uchimura et al., 2010; Abhirup et al., 2018; Xie et al., 2019). This technique is employed to detect the abnormal tilting of the slope surface before the occurrence of slope failure. The criteria for early warning using tilt sensors were first introduced by Uchimura et al. (2015) based on physical and field tests, which were shown to be conservative (Xie et al., 2020). Subsequently, a more efficient and accurate landslide prediction method using pre-failure tilting behavior was proposed by Xie et al. (2020), which has been employed to forecast the failure time of landslides in field events. Although the proposed method has been validated by physical models and field cases (Xie et al., 2020), it is still challenging to obtain exact slope failure time because of the uncertainties in monitoring data caused by environmental noise (e.g. weather, fluctuations in sensors and land surface flora and fauna activity), measurement errors, and inherent unpredictability in slope behavior. In addition, the surface tilting method utilizes the least squares method to estimate failure time and thus cannot provide a confidence interval for failure time, which is crucial for reliable field predictions by governments and researchers.

The Bayesian approach has been employed to account for observational errors in slope monitoring data and uncertainties in prediction models. This method integrates prior information with monitoring data to obtain posterior information and infer unknown parameters. The Bayesian approach has been used to estimate slope failure time using the inverse velocity method (Zhang et al., 2020; Zhang et al., 2022; Lacroix et al., 2023; Zhou et al., 2024). However, few studies have been found to apply a Bayesian approach to landslide prediction models using surface tilting data (Wang et al., 2022a, 2022b; Liu et al., 2023). In addition, the dynamic update of landslides using forecasting models can significantly improve prediction reliability, but such research is still sparse.

To address these limitations, this paper aims to develop a dynamic prediction model using tilting measurements to predict slope failure time intervals while considering observational errors through Bayesian linear regression. The proposed method was assessed through three physical-scale tests and compared to conventional forecast model. This method was then applied to a total of fifteen tests to establish the relationship between prediction errors and the percentage of input data.

2. Theoretical background and methodology

2.1. Conventional landslide prediction model using surface tilting

Slope deformation typically consists of three stages as shown in Fig. 1: (1) a primary phase, characterized by a decreasing strain rate over time; (2) a secondary phase with constant strain rate; and (3) an accelerating phase, marked by a rapid increase in the strain rate until to failure (Augustesen et al., 2004). Since slope deformation over time prior to failure often takes place in the accelerating phase, many prediction methods are applied to this stage (Federico et al., 2012; Federico et al., 2015). The conventional landslide prediction model using surface tilting in accelerating phase was proposed by Xie et al. (2020):

$$\frac{dt}{d\theta} = \frac{-t}{B} + \frac{t_f}{B} \quad (1)$$

where $\frac{dt}{d\theta}$ is the inverse tilting rate in the accelerating phase; t is time; B is the angular coefficient derived from the linear relationship between the reciprocal tilting rate and time; and t_f is the slope failure time. In this model, the tilting angle θ is considered as deformation and used in this classical linear method to predict failure time, which is shown by a scatter plot in Fig. 1. By integrating with regard to time, Eq. (1) can be re-written as:

$$\theta = -\ln B(t_f - t) + C \quad (2)$$

where θ is the tilting angle in the accelerating phase, C is a constant. The tilting angle is measured by tilting sensors. Due to uncertainties, such as measurement errors and environmental noise, the predicted and actual curves are different in the accelerating phase, as shown in Fig. 1.

Tilting sensors used in this paper for slope tilting measurement are described by (Uchimura et al., 2015; Wang et al., 2022a, 2022b). Surface tilting sensors equipped with MEMS technique to measure the variety of angel in slope and the nominal resolution was $0.0025^\circ = 0.04 \text{ mm/m}$.

2.2. New failure time forecasting method based on the Bayesian approach

In this research, Bayesian linear regression (Smith, 1973; Walter and Augustin, 2010) is used to estimate slope failure time. Considering observational errors, Eq. (1) is re-written as:

$$t = t_f - BR + \varepsilon_o \quad (3)$$

where R is the reciprocal of the angular tilting rate; and ε_o is the observational error, represented as a normal random variable with a mean of 0 and standard deviation of σ_o .

Let t_{Nf} , B_N , and σ_{No}^2 denote t_f , B , and σ_o^2 , of a new slope, respectively, which are considered to be uncertain in this study. Let vector $\lambda = (t_{Nf}, -B_N)^T$, and assume that at time t_{Ni} , the observed reciprocal of the tilting rate is R_{Ni} . For simplicity, t_{Ni} and R_{Ni} are expressed in vector form. Using $\mathbf{t}_N = (t_{N1}, t_{N2}, \dots, t_{Nn})^T$ and $\mathbf{R}_N = (R_{N1}, R_{N2}, \dots, R_{Nn})^T$, given known \mathbf{R}_N, λ and σ_{No}^2 , the likelihood function is expressed as:

$$L(\mathbf{t}_N | \mathbf{R}_N, \lambda, \sigma_{No}^2) = \prod_{i=1}^{n_N} \phi\left(\frac{t_{Ni} - t_{Nf} + B_N R_{Ni}}{\sigma_{No}}\right) \quad (4)$$

where ϕ is the probability density function of the standard normal. Conjugate prior distributions are considered to simplify the calculation (Del Castillo, 2007; Walter and Augustin, 2010). In this study, the conjugate prior distributions for σ_{No}^2 follows a scaled inverse chi-squared distribution, and λ follows a multivariate normal distribution:

$$f(\sigma_{No}^2) = \text{Scale} - \text{Inv} - \chi^2(\nu_0, s_0^2) \quad (5)$$

$$f(\lambda | \sigma_{No}^2) = \text{MVNormal}(\mu_0, \sigma_{No}^2 A_o^{-1}) \quad (6)$$

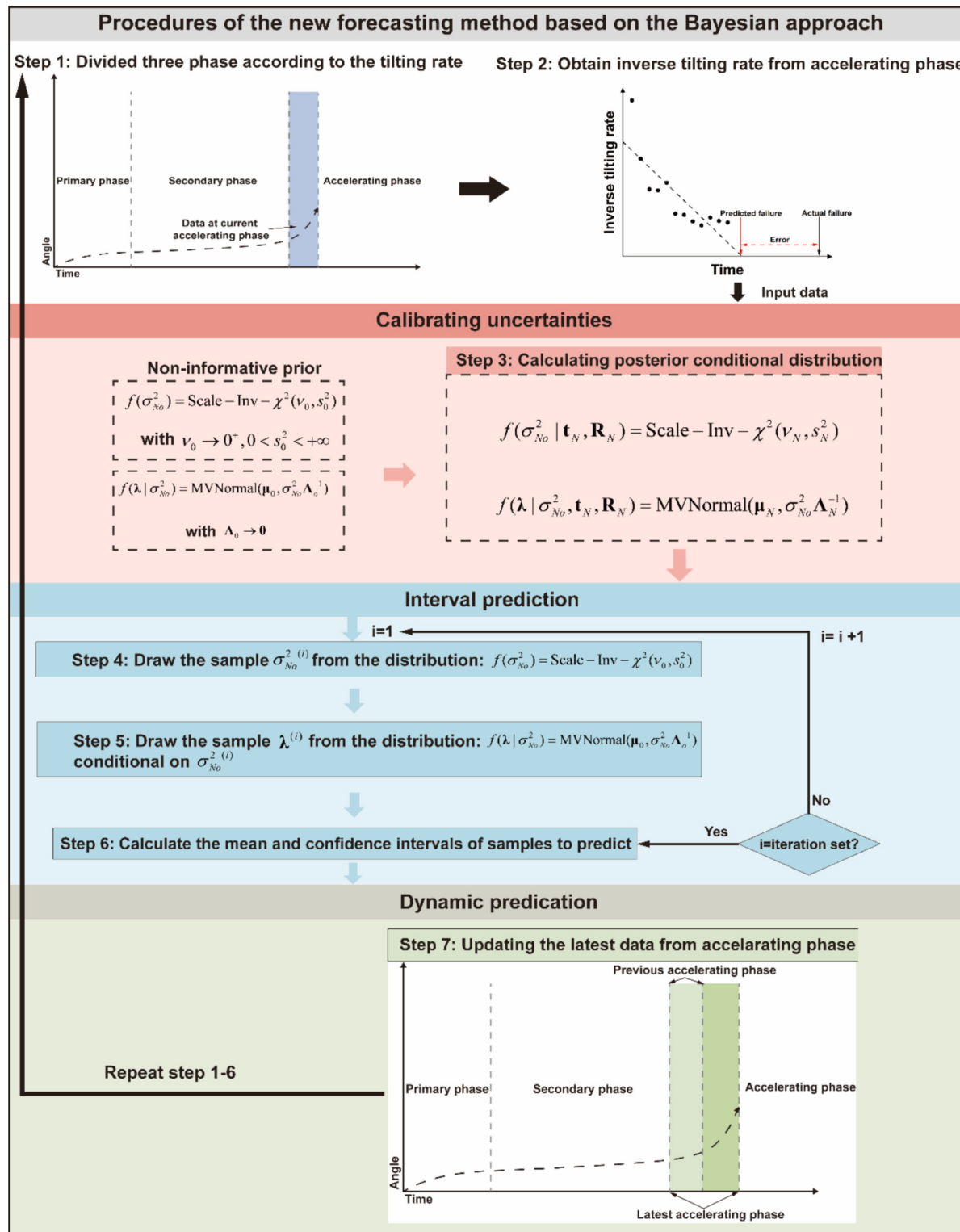


Fig. 2. Flowchart of the new Bayesian forecasting method.

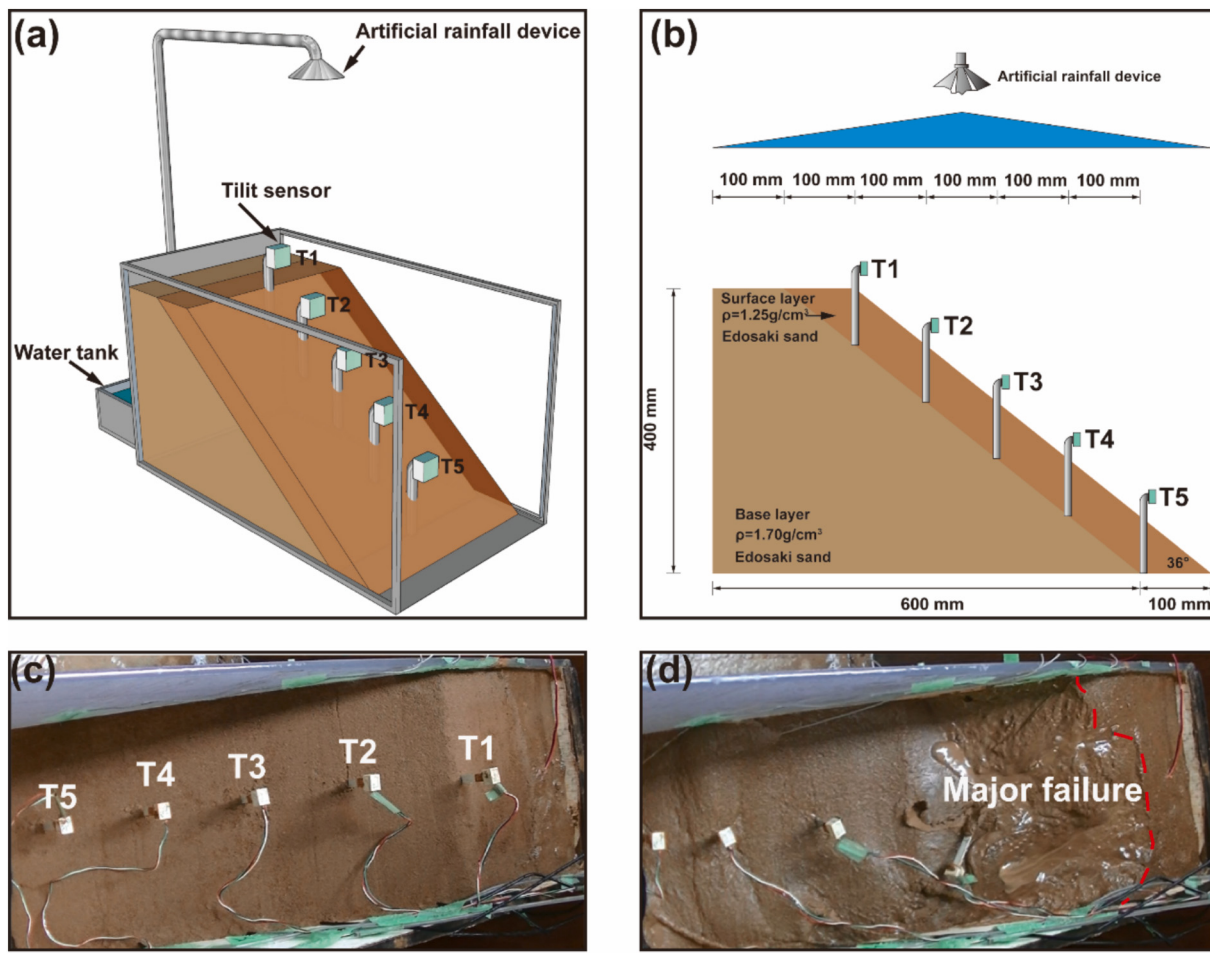


Fig. 3. Model test configurations: (a) 3-D experimental setup, (b) Side view, (c) Tilt sensor locations, (d) Slope failure.

where ν_0 is the degree of freedom; and s_0^2 is the scale parameter for the scaled inverse chi-squared distribution; and μ_0 and $\sigma_{N_0}^2 \Lambda_0^{-1}$ represent the mean and covariance matrix of the multivariate normal distribution, respectively. In practical Bayesian applications, a large amount of data is usually required to obtain reliable prior distributions. Since sufficient data for slope failure time predictions are often unavailable, a non-informative prior distribution will be used in this study (Gelman et al., 2013). When $\nu_0 \rightarrow 0^+, 0 < s_0^2 < +\infty$, and $\Lambda_0 \rightarrow \mathbf{0}$, the prior distributions of $\sigma_{N_0}^2$ and λ can be considered to be non-informative.

The posterior distribution of λ can be calculated as (Korner-Nievergelt et al., 2015):

$$f(\sigma_{N_0}^2 | \mathbf{t}_N, \mathbf{R}_N) = \text{Scale} - \text{Inv} - \chi^2(\nu_N s_N^2) \quad (7)$$

$$f(\lambda | \sigma_{N_0}^2, \mathbf{t}_N, \mathbf{R}_N) = \text{MVNormal}(\mu_N \sigma_{N_0}^2 \Lambda_N^{-1}) \quad (8)$$

where $\mu_N = (\mathbf{X}^T \mathbf{X} + \Lambda_0)^{-1} (\Lambda_0 \mu_0 + \mathbf{X}^T \mathbf{X} \hat{\lambda})$; $\Lambda_N = \mathbf{X}^T \mathbf{X} + \Lambda_0$; $\nu_N = \nu_0 + (n_N - p)$; $s_N^2 = \frac{\nu_0}{\nu_N} s_0^2 + \frac{1}{\nu_N} (\mathbf{t}_N^T \mathbf{t}_N + \mu_0^T \Lambda_0 \mu_0 - \mu_N^T \Lambda_N \mu_N)$; $\hat{\lambda} = (\mathbf{X}^T \mathbf{X})^{-1} \mathbf{X}^T \mathbf{t}_N$; and p is the dimension of λ , which equals 2 in this paper. \mathbf{X}_N is called the design matrix (Castillo et al., 2015), as shown by Eq. (9).

$$\mathbf{X}_N = \begin{pmatrix} 1 & R_{N1} \\ 1 & R_{N2} \\ \vdots & \vdots \\ 1 & R_{Nn} \end{pmatrix} \quad (9)$$

To obtain samples of the posterior distribution, a Markov-chain

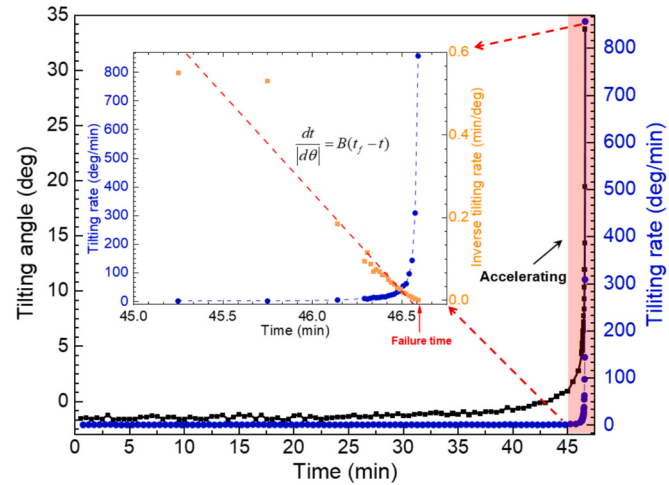


Fig. 4. Time series of the tilting angle and inverse tilting rate of T5.

Monte Carlo (MCMC) method, such as the Gibbs sampler, was used in this study (e.g., Wang and Luo, 2013; Ering and Babu, 2016; Wang et al., 2020; Geman and Geman, 1984; Zhang et al., 2023). The detailed procedures of the new Bayesian forecasting method are described in Fig. 2.

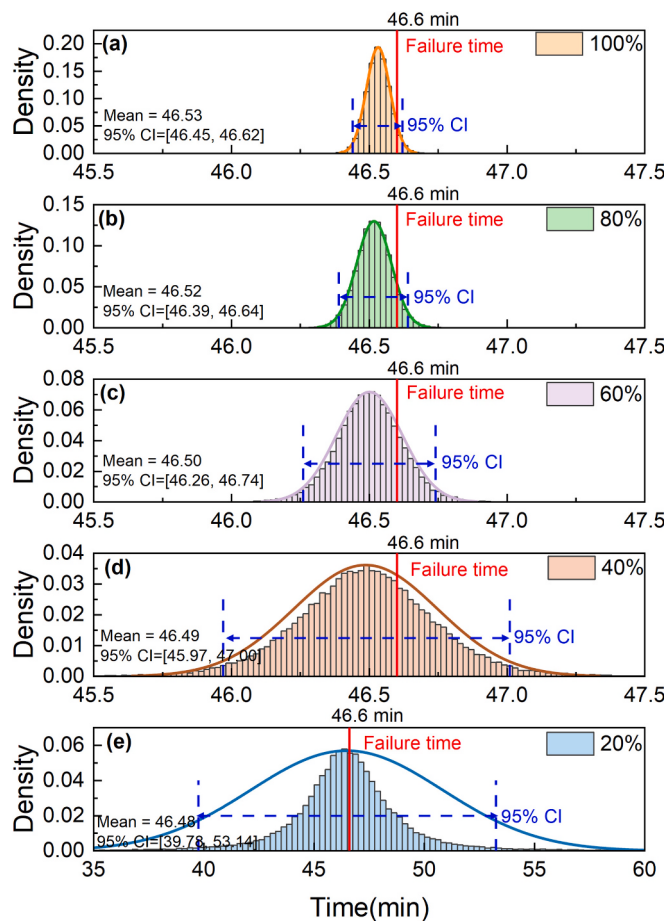


Fig. 5. Predicted failure time using the Bayesian approach with different percentages of input data in the model test: (a) 100 % tilting rate data, (b) 80 % tilting rate data, (c) 60 % tilting rate data, (d) 40 % tilting rate data, (e) 20 % tilting rate data.

3. Verification and results

3.1. Model test

The slope model illustrated in Fig. 3 was constructed using Edosaki Sand sourced from a natural slope in Ibaraki Prefecture, Japan. In this model, the base and surface layers had initial water contents of 14.6 % and 10 %, respectively. The specific gravity (G_s) of the sand was 2.68. The permeability of the surface layer was 4.70×10^{-3} cm/s, while that of the base layer was less than 1×10^{-3} cm/s. The 100-mm-thick surface layer contained five tilt sensors horizontally installed at 100 mm intervals on the 36° slope, as shown in Fig. 3. Slope failure was triggered by applying artificial rainfall at a constant intensity of 70 mm/h (Xie et al., 2020).

In this test, T5 measured the first slope failure in the progressive failure process. In the progressive failure, we think the first failure can be seen as the failure occurrence in slope. Therefore, the tilting angle data from sensor T5 in the accelerating phase were used to validate the proposed method. Fig. 4 illustrates the tilting angle, tilting rate, and inverse tilting rate of T5 during the acceleration phase. The first measurement was taken at time $t = 0$, and the acceleration phase began at $t = 45$ mins, with the failure occurring at $t = 46.6$ mins. In this test, the slope deformation directly entered the secondary phase and then started

accelerating.

The proposed method generated 1×10^5 posterior samples using the Gibbs sampler, with the initial 5×10^4 samples discarded as burn-in to ensure Markov chain convergence. Fig. 5 presents the failure time predictions, including probability density, predicted mean, and 95 % confidence intervals. Dynamic predictions were performed using 20 %, 40 %, 60 %, 80 %, and 100 % of the tilting data in the accelerating phase. The mean of the posterior samples approaches the actual failure time (i.e., $t_f = 46.6$ mins) as the percentage of data increases. Particularly, the mean for the 100 % data case is 46.53 mins, with an error of just 0.14 %. Additionally, the 95 % confidence interval narrows gradually with the increase of the input percentage, and the actual failure time is well within this interval. This demonstrates that the prediction accuracy and reliability improve with more input data, as expected. Unlike conventional models, this approach is able to quantify prediction uncertainty through confidence intervals.

3.2. Field test

Compared to model tests, field tests have larger physical scales and are closer to actual geological situations. In this study, a field test was performed on a natural slope in Baise city, Guangxi Province, China. The natural slope was composed of weakly expansive clay. The slope angle was approximately 40°, and its high stability at this steep angle was attributed to the robust structure of the expansive clay. To facilitate a potential collapse, a trench was excavated at the toe of the slope to a depth of 0.2 m. For more details of this slope, refer to Xie et al. (2020). Six tilt sensors were installed in the slope, as illustrated in Fig. 6. Artificial rainfall was applied at a constant intensity of 27 mm/h, resulting in a major failure occurred in the middle part of the slope after approximately four hours.

In this test, the major failure region was located in the middle of the slope, and only sensor T3 monitored the tilting data in failure area. Hence, the data from sensor T3 was utilized to validate the proposed method. The number of posterior samples generated was the same as that for the model test. Fig. 7 illustrates the tilting angle, tilting rate, and inverse tilting rate of T3 in the accelerating phase. $t = 0$ represents the time when the first measurement was recorded. The accelerating phase started at $t = 75.01$ mins, and the failure occurred at $t = 88.27$ mins, see Fig. 8.

In the field test, there is a similar trend compared to the model test, with the prediction accuracy increasing as the volume of input data grows. Specifically, using 100 % of the data, the mean predicted failure time is 88.2 min (error of 0.08 %), outperforming the model test case. Moreover, the 95 % confidence interval narrows progressively with increasing input data percentage and consistently captures the actual failure time. These field results further demonstrate the practical robustness of the proposed Bayesian prediction approach.

3.3. Field monitoring

This section focuses on a significant slope failure that occurred alongside National Highway 500 in Fukuoka Prefecture, Japan, during the tumultuous weather caused by Typhoon No. 11, known as “Nangka”. The failure was triggered by the intense rainfall associated with the typhoon on July 17–18, 2015. The affected slope is primarily composed of Funi volcanic rock, featuring andesite karst, tuff breccia, and tuff. More details and properties of this slope can be found in Wang et al. (2022a, 2022b). To maintain traffic during slope restoration, the slope movement was monitored using a set of tilt sensors, as shown in Fig. 9.

For this case, the data from sensor K-2 were considered to examine

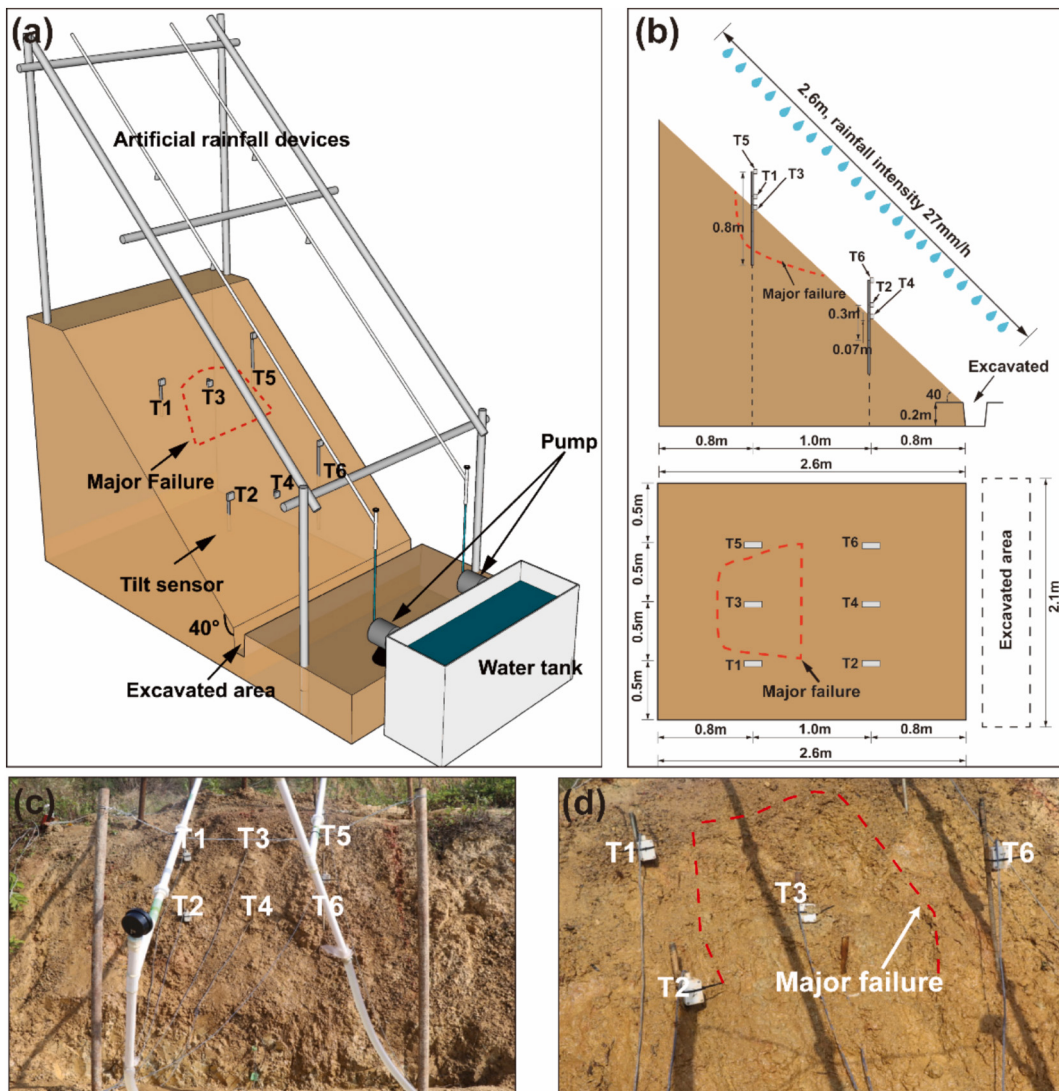


Fig. 6. Field test configurations: (a) 3-D experimental setup, (b) Side and Top view, (c) Sensor locations, (d) Slope failure.

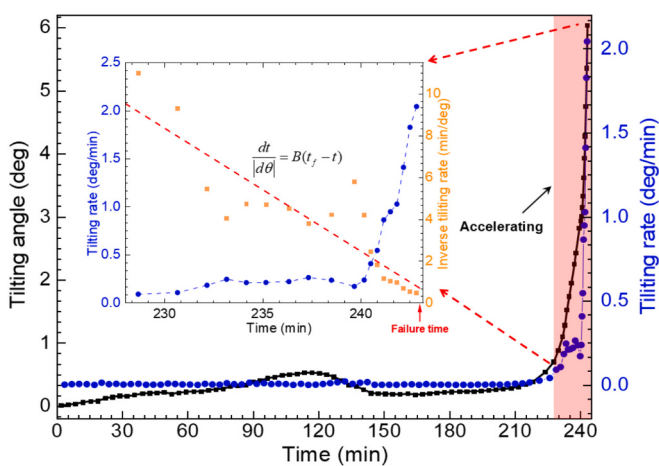


Fig. 7. Time series of tilting angle and inverse tilting rate in the field test.

the proposed method because this sensor firstly measured the slope failure occurrence. The number of posterior samples generated were same as in the previous examples. Fig. 10 displays the tilting angle, tilting rate, and inverse tilting rate of sensor K-2 on July 21st and 22nd, shortly after the main slope collapse. $t = 0$ represents the time when the first measurement was recorded. The accelerating phase of this slope started at $t = 1007$ mins, and the failure occurred at $t = 1252$ mins.

Similarly, the 20 %, 40 %, 60 %, 80 %, and 100 % of the data from the accelerating phase were selected to make predictions. As shown in Fig. 11, when insufficient data were input (20 %–60 %), the predicted failure times significantly deviate from the actual failure time, and the 95 % confidence intervals fail to capture the actual failure time. With more data incorporated, the predicted mean becomes progressively closer to the actual failure time, and the 95 % confidence interval narrows gradually. With 100 % of the data, the actual failure time falls well within the 95 % confidence interval, and the predicted mean failure time is 1248.82 mins with an error of only 0.02 %. This indicates that though the initial results may be inaccurate due to the complex geological and environmental conditions, the proposed Bayesian prediction approach is

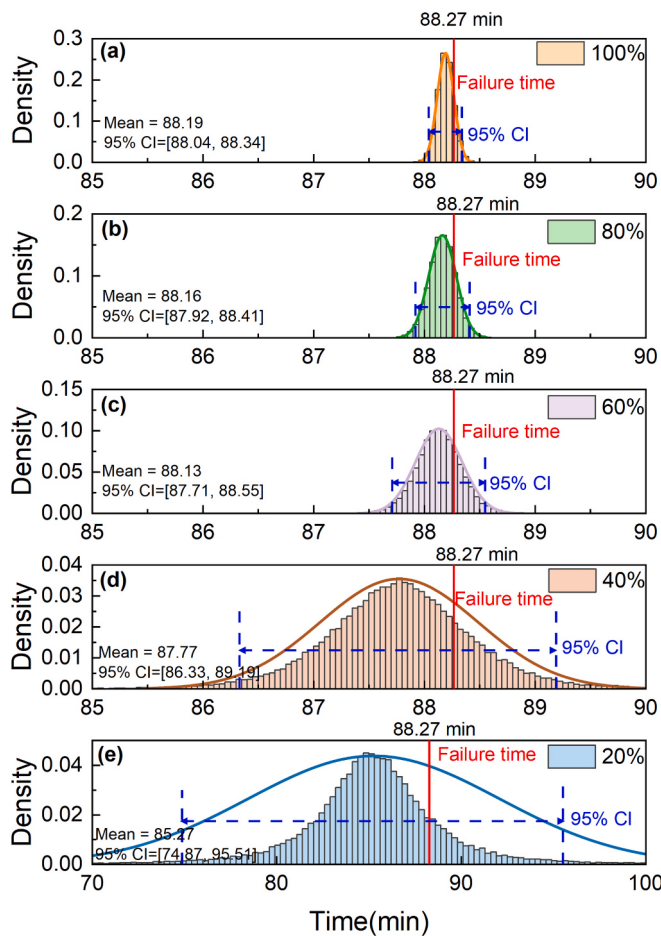


Fig. 8. Predicted failure time with different percentages of input data in the field test: (a) 100 % tilting rate data, (b) 80 % tilting rate data, (c) 60 % tilting rate data, (d) 40 % tilting rate data, (e) 20 % tilting rate data.

still capable of providing sufficiently accurate failure time interval predictions with an increased volume of data input.

4. Discussion

4.1. Comparison between conventional and current prediction models

This section compares the proposed Bayesian method with the classical linear forecasting approach (Xie et al., 2020) for slope failure time prediction using tilt measurements. The comparison employs the three case study datasets from Section 3, with results presented in Fig. 12.

The 99 %, 95 % and 85 % confidence intervals are calculated from the posterior samples for the three illustrative examples respectively.

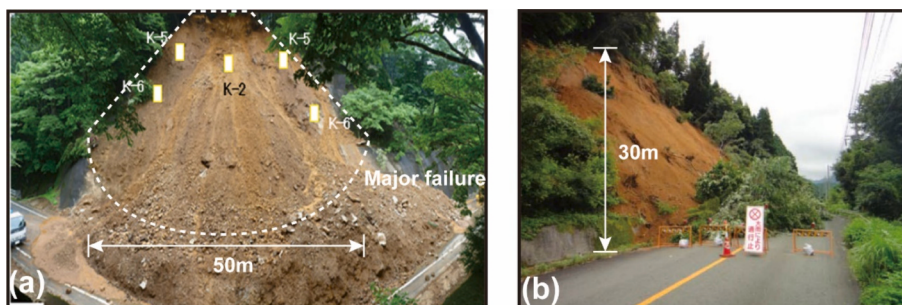


Fig. 9. Field monitoring: (a) Sensor locations, (b) Slope failure.

The figures show that both the traditional and current methods provide failure times close to the actual failure time (red dash lines) with an increasing percentage of input data. However, the new Bayesian prediction model provides better predictions than the conventional model. It is also noted that the failure time predicted by the conventional model lies outside the lower boundary of the 95 % confidence intervals and nearly matches the lower bound of the 99 % confidence intervals. The comparative analysis reveals that the classical linear method (or point prediction) provides less comprehensive predictions with relatively larger errors than proposed Bayesian prediction model.

4.2. Relationship between prediction errors and quantity of input data

The proposed method is further applied to 12 additional tests, including scaled physical model tests, full-scale field tests, and field monitoring. The tilting angle data from the accelerating phase of the 12 tests are shown in Fig. 13, and Table 1 summarize the prediction results from all 15 tests.

The accuracy of the predicted failure time is estimated using the following equation:

$$E = \frac{t_m - t_a}{t_s - t_a} \% \quad (10)$$

where E is the error between the predicted mean time and actual time; t_m is the mean of posterior samples; t_a is the actual failure time; and t_s is the start time of the accelerating phase. The predication errors of these tests calculated by Eq. (10) with different percentages of input data are shown in Fig. 14. Notably, the illustrative examples of model test, field test and field monitoring are named Edosaki Sand Model Test, Guanxi Field Test 1 and Failed Slope in Fukuoka in Fig. 14, respectively.

The following equation is used to fit the mean, upper and lower 95 %

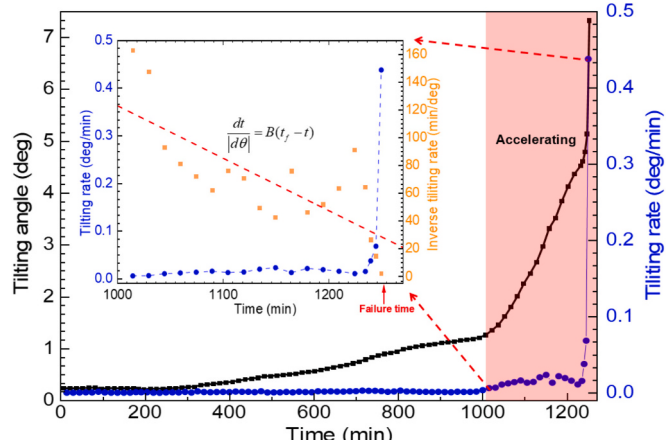


Fig. 10. Time series of tilting angle and inverse tilting rate in the field monitoring.

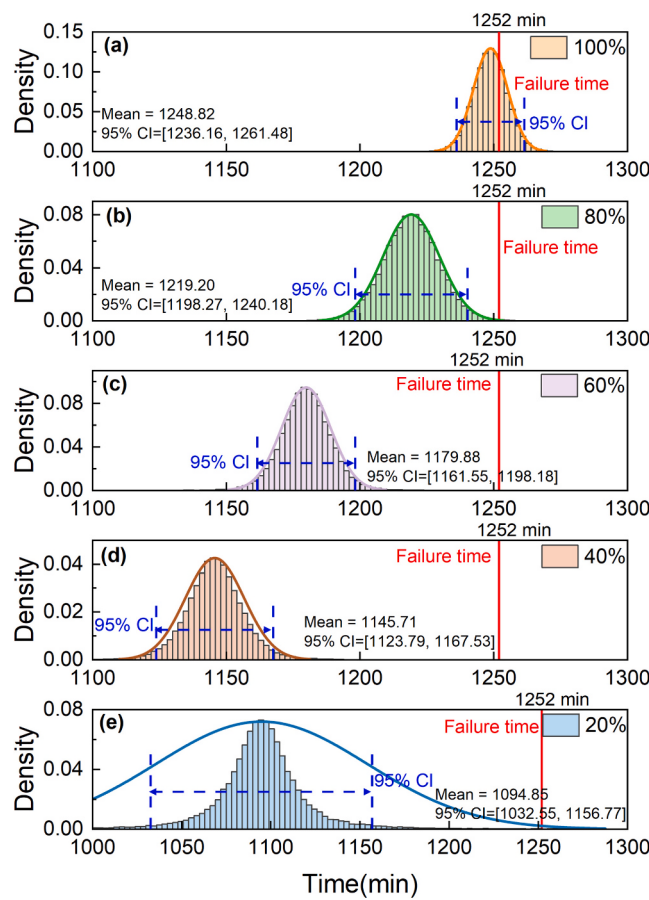


Fig. 11. Predicted failure time with different percentages of input data in the field monitoring: (a) 100 % tilting rate data, (b) 80 % tilting rate data, (c) 60 % tilting rate data, (d) 40 % tilting rate data, (e) 20 % tilting rate data.

confidence intervals, i.e.,

$$y = y_0 + A_1 \exp\left(\frac{-x}{t_1}\right) \quad (11)$$

where y_0 , A_1 , t_1 are regression coefficients. In Fig. 14, the mean is shown by the solid line and the upper and lower 95 % confidence intervals are shown by the dashed lines.

The figure illustrates that as the percentage of input data increases, the mean prediction error and the confidence bounds decrease, as expected. The lower bound of the 95 % confidence interval remains relatively stable below 20 %, while the upper bound decreases significantly from 100 % to nearly 20 %, indicating that the mean, upper, and lower bounds converge as the volume of input data increases.

The relationship between the failure prediction error and the amount of input data provides an important insight into the performance of the prediction model. Fig. 14 shows that dynamic predictions based on the Bayesian forecasting method gradually become more accurate and reliable as more data becomes available. Nevertheless, the predicted failure time still shows a great discrepancy in the early stages with limited data available. It is worth noting that the proposed method is not applicable to slope failures with multiple accelerating phases or those without a clear accelerating phase. Also, it requires considerable computational resources for real-time calculations.

5. Conclusions

Landslide prediction models using surface tilting are widely used to predict slope failure time. However, factors such as measurement errors

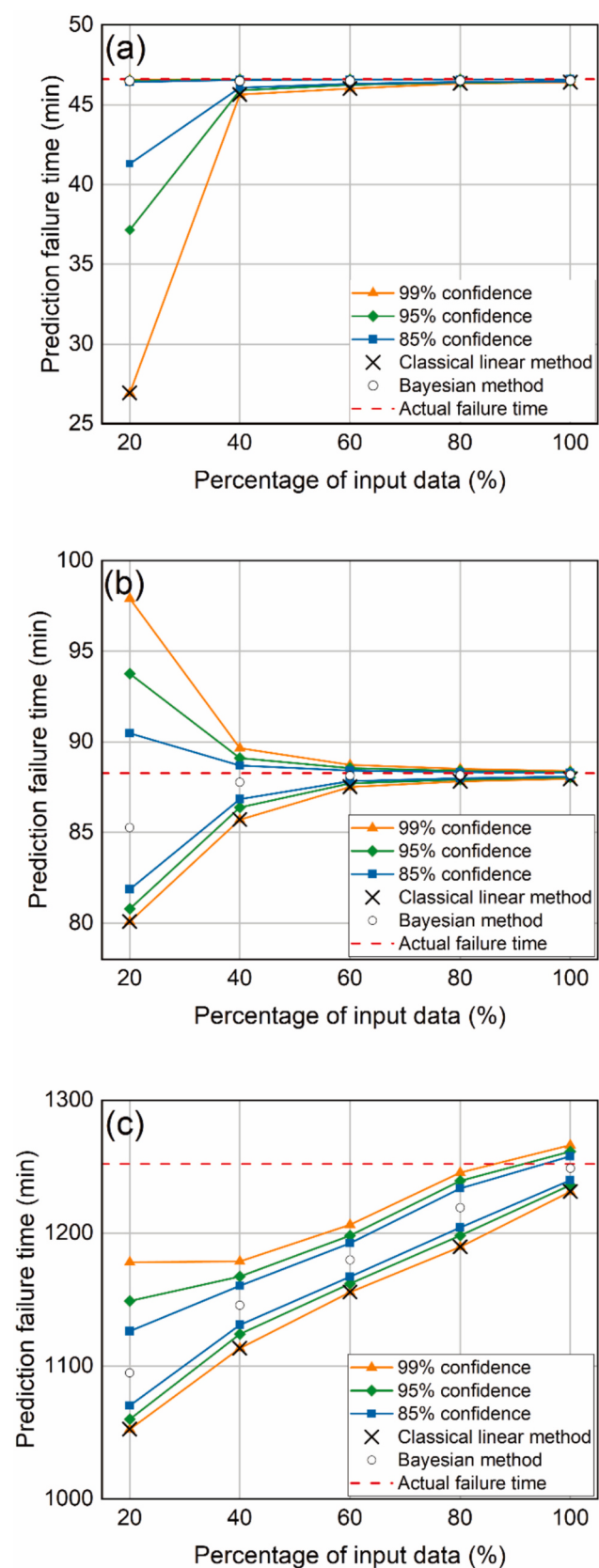


Fig. 12. Comparison between conventional and current prediction models: (a) model test, (b) field test, (c) field monitoring.

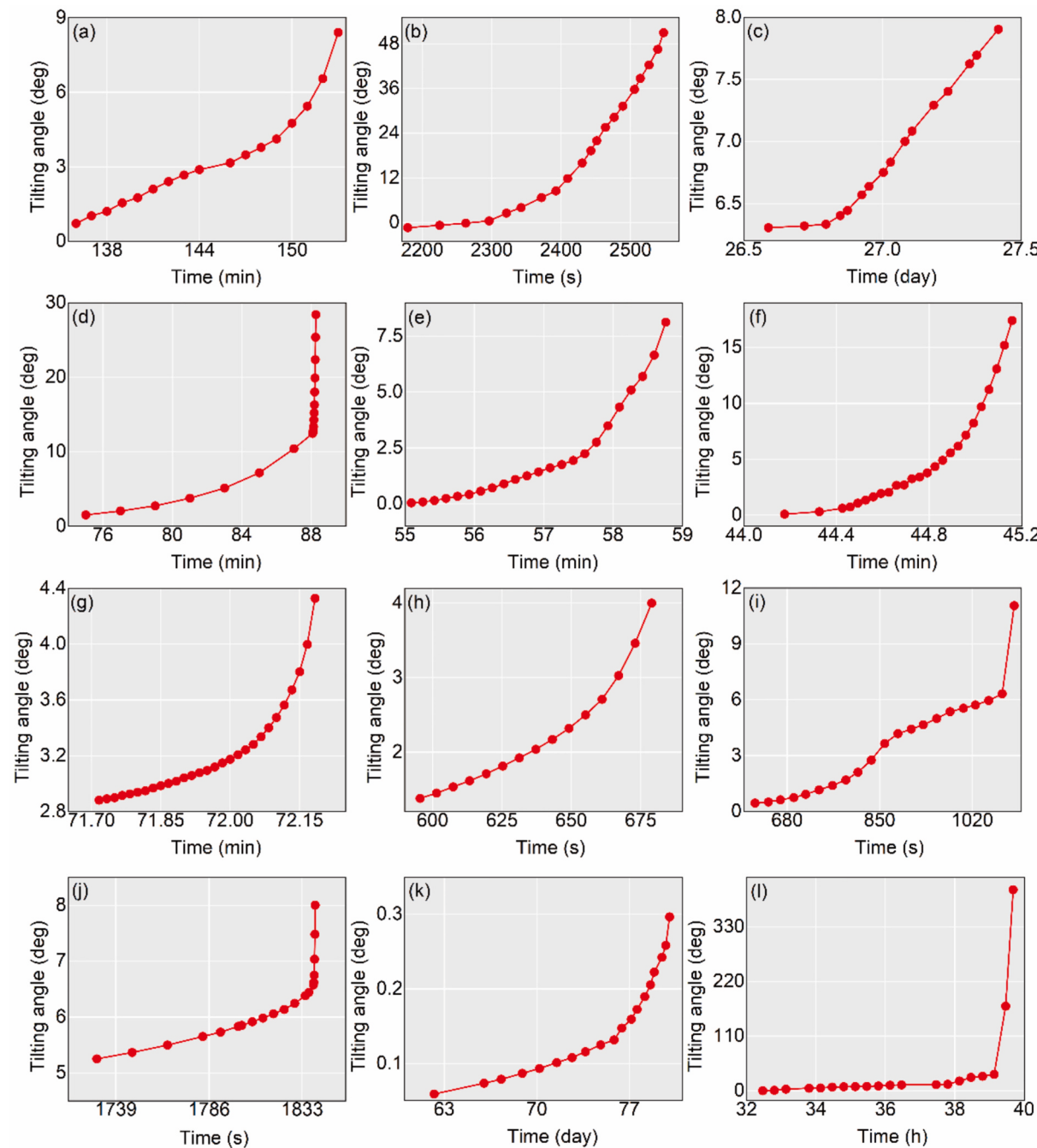
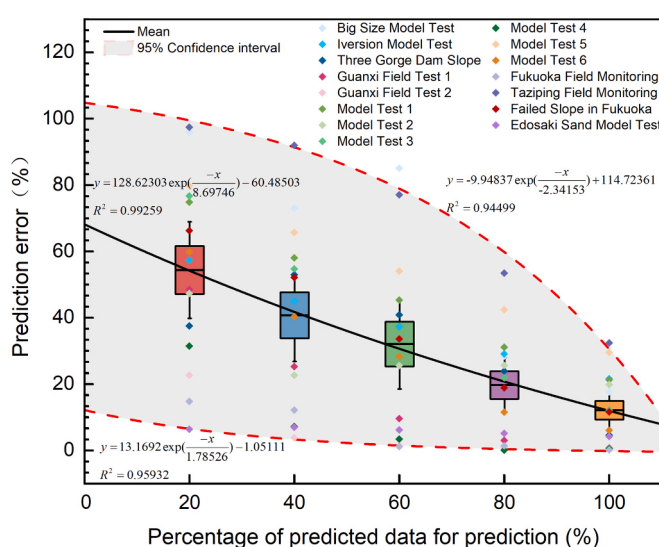


Fig. 13. Tilting angle data in accelerating phase versus time: (a) Big Size Model Test (Adapted from Uchimura et al., 2011; Xie et al., 2020), (b) Iverson Model Test (Adapted from Iverson et al., 2000), (c) Three Gorge Dam Slope (Adapted from Uchimura et al., 2015), (d) Guanxi Field Test 2 (Adapted from Xie et al., 2020), (e) Model Test 1, (f) Model Test 2, (g) Model Test 3, (h) Model Test 4, (i) Model Test 5, (j) Model Test 6, (k) Fukuoka Field Monitoring (Adapted from Uchimura et al., 2015), (l) Taziping Field Monitoring (Adapted from Uchimura et al., 2015).

Table 1

Predictions from 15 tests.

Test name	Actual failure time	20 % data	40 % data	60 % data	80 % data	100 % data	Source
Big Size Model Test	154 min	Mean: 137.21 min 95 % CI: [120.78, 153.56] min	Mean: 141.22 min 95 % CI: [136.35, 146.00] min	Mean: 139.12 min 95 % CI: [136.20, 142.02] min	Mean: 149.03 min 95 % CI: [147.36, 150.71] min	Mean: 150.92 min 95 % CI: [149.77, 152.08] min	Uchimura et al., 2011
Iversion Model Test	2547 s	Mean: 2336 s 95 % CI: [2245, 2426] s	Mean: 2382 s 95 % CI: [2366, 2397] s	Mean: 2410 s 95 % CI: [2421, 2399] s	Mean: 2440 s 95 % CI: [2431, 2449] s	Mean: 2468 s 95 % CI: [2460, 2476] s	Iverson et al., 2000
Three Gorge Dam Slope	27.44 day	Mean: 27.20 day 95 % CI: [27.50, -72.60] day	Mean: 27.10 day 95 % CI: [24.07, 30.20] day	Mean: 27.18 day 95 % CI: [25.76, 28.59] day	Mean: 27.29 day 95 % CI: [26.47, 28.11] day	Mean: 27.47 day 95 % CI: [26.94, 28.00] day	Uchimura et al., 2015
Guanxi Field Test 1 (Illustrative field test)	88.27 min	Mean: 85.27 min 95 % CI: [74.87, 95.51] min	Mean: 87.77 min 95 % CI: [86.33, 89.19] min	Mean: 88.13 min 95 % CI: [87.71, 88.55] min	Mean: 88.16 min 95 % CI: [87.92, 88.41] min	Mean: 88.19 min 95 % CI: [88.04, 88.34] min	Xie et al., 2020
Guanxi Field Test 2	243.00 min	Mean: 235.57 min 95 % CI: [225.20, 246.06] min	Mean: 239.13 min 95 % CI: [237.29, 240.97] min	Mean: 241.54 min 95 % CI: [239.75, 243.32] min	Mean: 242.55 min 95 % CI: [241.76, 243.33] min	Mean: 242.89 min 95 % CI: [242.46, 243.32] min	Xie et al., 2020
Model Test 1	58.76 min	Mean: 55.89 min 95 % CI: [46.25, 65.53] min	Mean: 56.54 min 95 % CI: [55.78, 57.28] min	Mean: 57.02 min 95 % CI: [56.64, 57.40] min	Mean: 57.57 min 95 % CI: [57.37, 57.77] min	Mean: 57.95 min 95 % CI: [57.81, 58.08] min	–
Model Test 2	45.16 min	Mean: 45.62 min 95 % CI: [0.00, 91.50] min	Mean: 44.94 min 95 % CI: [37.10, 52.83] min	Mean: 44.91 min 95 % CI: [41.01, 48.81] min	Mean: 44.91 min 95 % CI: [42.80, 47.03] min	Mean: 44.96 min 95 % CI: [43.61, 46.33] min	–
Model Test 3	72.18 min	Mean: 71.83 min 95 % CI: [67.97, 75.69] min	Mean: 71.93 min 95 % CI: [71.18, 72.68] min	Mean: 72.03 min 95 % CI: [71.73, 72.33] min	Mean: 72.08 min 95 % CI: [71.93, 72.24] min	Mean: 72.13 min 95 % CI: [72.04, 72.21] min	–
Model Test 4	688 s	Mean: 658 s 95 % CI: [0, 1330] s	Mean: 681 s 95 % CI: [667, 695] s	Mean: 691 s 95 % CI: [687, 696] s	Mean: 688 s 95 % CI: [686, 690] s	Mean: 688 s 95 % CI: [687, 689] s	–
Model Test 5	1097 s	Mean: 717 s 95 % CI: [665, 790] s	Mean: 784 s 95 % CI: [763, 805] s	Mean: 840 s 95 % CI: [822, 858] s	Mean: 895 s 95 % CI: [873, 917] s	Mean: 956 s 95 % CI: [935, 978] s	–
Model Test 6	1840 s	Mean: 1906 s 95 % CI: [1828, 1983] s	Mean: 1884 s 95 % CI: [1871, 1897] s	Mean: 1871 s 95 % CI: [1866, 1876] s	Mean: 1852 s 95 % CI: [1850, 1855] s	Mean: 1846 s 95 % CI: [1845, 1848] s	–
Fukuoka Field Monitoring	80.04 day	Mean: 82.66 day 95 % CI: [51.29, 113.70] day	Mean: 82.19 day 95 % CI: [78.65, 85.74] day	Mean: 80.25 day 95 % CI: [79.09, 81.41] day	Mean: 79.80 day 95 % CI: [79.23, 80.38] day	Mean: 80.05 day 95 % CI: [79.75, 80.36] day	Uchimura et al., 2015
Failed Slope in Fukuoka (Illustrative field monitoring)	1252 min	Mean: 1094.85 min 95 % CI: [1032.55, 1156.77] min	Mean: 1145.71 min 95 % CI: [1123.79, 1167.53] min	Mean: 1179.88 min 95 % CI: [1161.55, 1198.18] min	Mean: 1219.20 min 95 % CI: [1198.27, 1240.18] min	Mean: 1248.82 min 95 % CI: [1236.16, 1261.48] min	Wang et al., 2022a, 2022b
Edosaki Sand Model Test (Illustrative model test)	46.6 min	Mean: 46.48 min 95 % CI: [39.78, 53.14] min	Mean: 46.49 min 95 % CI: [45.97, 47.00] min	Mean: 46.50 min 95 % CI: [46.26, 46.74] min	Mean: 46.52 min 95 % CI: [46.39, 46.64] min	Mean: 46.53 min 95 % CI: [46.45, 46.62] min	Xie et al., 2020

**Fig. 14.** Prediction errors with different percentages of input data across 15 tests.

and environmental noise can result in considerable errors in the predicted failure time. This paper proposed a new failure time forecasting method using a Bayesian approach based on slope surface tilting measurements. The main contributions are summarized as follows:

- (1) A new Bayesian prediction model for estimating slope failure time was proposed. It can provide accurate real-time forecasting of failure time intervals while accounting for observational uncertainties in the monitoring data.
- (2) A Bayesian update approach was developed, combining non-informative prior distributions and the Markov-chain Monte Carlo (MCMC) method. This allows dynamic predictions of slope failure time with limited prior knowledge and complex posterior distributions.
- (3) A comparison was made between the new Bayesian and conventional prediction methods. The results show that the Bayesian method can provide a more robust and accurate predictions.
- (4) Regressive formulas with 95 % confidence were developed for the relationship between prediction errors and input data quantity using fifteen laboratory and field cases. They provide a valuable guidance for estimating prediction errors based on data availability.

CRediT authorship contribution statement

Nuo Chen: Writing – review & editing, Writing – original draft, Methodology, Investigation, Conceptualization. **Pengpeng He:** Writing – review & editing, Investigation. **Jiaxun Chen:** Writing – review & editing, Visualization. **Xiaocheng Huang:** Writing – review & editing. **Kun Fang:** Writing – review & editing. **Jiren Xie:** Writing – review & editing, Writing – original draft, Visualization, Methodology, Conceptualization. **Denis N. Gorobtsov:** Writing – review & editing, Conceptualization. **Margarita A. Novgorodova:** Writing – review & editing.

Funding declaration

The study was supported by National Natural Science Foundation of China (Grant no. 5220082708), Hunan Provincial Natural Science Foundation of China (Grant no. 2021JJ40764), the open project of Hunan Tieyuan Civil Engineering Testing Co., Ltd (Grant no. H202201260480001) and Science and Technology Research and Development Plan of China Railway Co., Ltd. (2022-Major Project-07).

Declaration of competing interest

The authors declare that they have no known competing financial interests or personal relationships that could have appeared to influence the work reported in this paper.

Acknowledgments

The authors would like to express the gratitude to the support of National Natural Science Foundation of China (Grant no. 5220082708), Hunan Provincial Natural Science Foundation of China (Grant no. 2021JJ40764), the open project of Hunan Tieyuan Civil Engineering Testing Co., Ltd. (Grant no. H202201260480001) and Science and Technology Research and Development Plan of China Railway Co., Ltd. (2022-Major Project-07).

Data availability statement

The data used to support the findings of this study are available from the corresponding author upon request.

References

- Abhirup, D., Satyam, D.N., Towhata, I., 2018. Early warning system using tilt sensors in Chibo, Kalimpong, Darjeeling Himalayas, India. *Nat. Hazards* 94, 727–741. <https://doi.org/10.1007/s11069-018-3417-6>.
- Al-Jawadi, A.S., 2024. Predicting slip surfaces for slope stability assessment along highway 80 in Mosul, Northern Iraq. *Geotech. Eng.* 42, 2997–3008. <https://doi.org/10.1007/s10706-023-02713-0>.
- Al-Jawadi, A.S., Al-Dabbagh, T.H., Dawlat, M.S., 2021. Slope assessment and suggested slope design of the behkme residential complex in North Iraq. *Indian Geotech. J.* 51, 694–704. <https://doi.org/10.1007/s40098-020-00497-1>.
- Augustesen, A., Liingaard, M., Lade, P.V., 2004. Evaluation of time-dependent behavior of soils. *Int. J. Geomech.* 4 (3), 137–156. [https://doi.org/10.1061/\(ASCE\)1532-3641\(2004\)4:3\(157\)](https://doi.org/10.1061/(ASCE)1532-3641(2004)4:3(157)).
- Bruland, C., Dichiarante, A.M., Köhler, A., Oye, V., Van Bever, I., Larose, E., 2025. Cultural activity and impact of extreme weather events revealed by ambient seismic noise and perspective on quick clay failure monitoring in Oslo, Norway. *Eng. Geol.*, 107936. <https://doi.org/10.1016/j.enggeo.2025.107936>.
- Castillo, I., Schmidt-Hieber, J., Van der Vaart, A., 2015. Bayesian linear regression with sparse priors. *Ann. Stat.* 43 (5), 1986–2018. <https://doi.org/10.1214/15-AOS1334>.
- Cui, Y., Li, Y., Tang, H., Turowski, J.M., Yan, Y., Wei, R., Li, L., 2024. A digital-twin platform for cryospheric disaster warning. *National Sci. Rev.*, nwae300 <https://doi.org/10.1093/nsr/nwae300>.
- Del Castillo, E., 2007. *Process Optimization: a Statistical Approach*. Springer, New York, NY, USA.
- Dixon, N., Smith, A., Flint, J.A., Khanna, R., Clark, B., Andjelkovic, M., 2018. An acoustic emission landslide early warning system for communities in low-income and middle-income countries. *Landslides* 15, 1631–1644. <https://doi.org/10.1007/s10346-018-0977-1>.
- Ering, P., Babu, G.L.S., 2016. Probabilistic back analysis of rainfall induced landslide—a case study of Malin landslide, India. *Eng. Geol.* 208, 154–164. <https://doi.org/10.1016/j.enggeo.2016.05.002>.
- Fan, Q., Zhang, S., Niu, Y., Zeng, X., Si, J., Li, X., Wu, W., Jiang, J., Qiu, S., Kang, Y., 2024. A non-contact quantitative risk assessment framework for translational highway landslides: Integration of InSAR, geophysical inversion, and numerical simulation. *Eng. Geol.* 107818. <https://doi.org/10.1016/j.enggeo.2024.107818>.
- Fang, K., Jia, S., Tang, H., Dong, A., Ding, B., An, P., Zhang, B., Miao, M., 2025. New insights into convergent slope instability: Physical modeling and stability analysis. *Eng. Geol.* 356, 108295. <https://doi.org/10.1016/j.enggeo.2025.108295>.
- Federico, A., Popescu, M., Elia, G., Fidelibus, C., Internò, G., Murianni, A., 2012. Prediction of time to slope failure: a general framework. *Environ. Earth Sci.* 66 (1), 245–256. <https://doi.org/10.1007/s12665-011-1231-5>.
- Federico, A., Popescu, M., Murianni, A., 2015. Temporal prediction of landslide occurrence: a possibility or a challenge. *Ital. J. Eng. Geol. Environ.* 1, 41–60. <https://doi.org/10.4408/IJEGE.2015-01.O-04>.
- Fukuzono, T., 1985. A new method for predicting the failure time of slopes. In: *In: Proceedings of the 4th International Conference & Field Workshop on Landslides, Tokyo*, pp. 145–150.
- Gelman, A., Stern, H.S., Carlin, J.B., Dunson, D.B., Vehtari, A., Rubin, D.B., 2013. *Bayesian Data Analysis*, third ed. Chapman and Hall/CRC, Boca Raton, FL, USA. <https://doi.org/10.1201/9780429258411>.
- Geman, S., Geman, D., 1984. Stochastic relaxation, Gibbs distributions, and the Bayesian restoration of images. *IEEE Trans. Pattern Anal. Mach. Intell.* 6 (6), 721–741. <https://doi.org/10.1109/TPAMI.1984.4767596>.
- Gong, Q.B., Yin, K.L., Xiao, C.G., Chen, L.X., Yan, L.X., Zeng, T.R., Liu, X.P., 2024. Double-index model of landslide meteorological warning based on the I-D threshold. *Bull. Geol. Sci. Technol.* 43 (1), 262–274. <https://doi.org/10.19509/j.cnki.dzkq.tb20220254>.
- Hao, S.W., Liu, C., Lu, C.S., Elsworth, D., 2016. A relation to predict the failure of materials and potential application to volcanic eruptions and landslides. *Sci. Rep.* 6, 27877. <https://doi.org/10.1038/srep27877>.
- Hu, X., Wu, S., Zhang, G., Zheng, W., Liu, C., He, C., Liu, Z., Guo, X., Zhang, H., 2021. Landslide displacement prediction using kinematics-based random forests method: a case study in Jinping Reservoir Area, China. *Eng. Geol.* 283, 105975. <https://doi.org/10.1016/j.enggeo.2020.105975>.
- Iverson, R.M., Reid, M.E., Iverson, N.R., LaHusen, R.G.L.M., Mann, J.E., Brien, D.L., 2000. Acute sensitivity of landslide rates to initial soil porosity. *Science* 290, 513–516. <https://doi.org/10.1126/science.290.5491.513>.
- Klose, M., Maurischat, P., Dann, B., 2016. Landslide impacts in Germany: a historical and socioeconomic perspective. *Landslides* 13 (1), 183–199. <https://doi.org/10.1007/s10346-015-0643-9>.
- Korner-Nievergelt, F., Roth, T., Von Felten, S., Guélat, J., Almasi, B., Korner-Nievergelt, P., 2015. *Bayesian Data Analysis in Ecology Using Linear Models with R, BUGS, and Stan*. Academic Press, Amsterdam, Netherlands.
- Lacroix, P., Huanca, J., Albinez, L., Taipe, E., 2023. Precursory motion and time-of-failure prediction of the Achoma Landslide, Peru, from high frequency PlanetScope satellites. *Geophys. Res. Lett.* 50, e2023GL105413. <https://doi.org/10.1029/2023GL105413>.
- Liu, H.D., Liu, J.J., Chen, J.X., Guo, Z.F., Qiu, Lei, 2023. Experimental study on tilting deformation and a new method for landslide prediction with retaining-wall locked segment. *Sci. Rep.* 13, 5149. <https://doi.org/10.1038/s41598-023-32477-9>.
- Lv, J., Zhang, R., Bao, X., Wu, R., Hong, R., He, X., Liu, G., 2025. Time-series InSAR landslides three-dimensional deformation prediction method considering meteorological time-delay effects. *Eng. Geol.* 107986. <https://doi.org/10.1016/j.enggeo.2025.107986>.
- Mufundirwa, A., Fujii, Y., Kodama, J., 2010. A new practical method for prediction of geomechanical failure-time. *Int. J. Rock Mech. Min. Sci.* 47 (7), 1079–1090. <https://doi.org/10.1016/j.ijrmms.2010.07.001>.
- Pang, X., Ming, Yuan, Yuan, Lu, Wenjie, Du, Daochun, Wan, De, Li, Haifeng, Ding, Xiaodong, Fu, 2023. Rapid identification method for the dangerous rock mass of a high-slope slope based on UAV LiDAR and ground imitation flight. *Bull. Geol. Sci. Technol.* 42 (6), 21–30. <https://doi.org/10.19509/j.cnki.dzkq.tb20220427>.
- Petley, D.N., 2012. Global patterns of loss of life from landslides. *Geology* 40 (10), 927–930. <https://doi.org/10.1130/G33217.1>.
- Petley, D.N., Mantovani, F., Bulmer, M.H., Zannoni, A., 2005. The use of surface monitoring data for the interpretation of landslide movement patterns. *Geomorphology* 66 (1–4), 133–147. <https://doi.org/10.1016/j.geomorph.2004.09.011>.
- Saito, M., 1965. Forecasting the time of occurrence of a slope failure. In: *In: Proceedings of the 6th International Conference on Soil Mechanics and Foundation Engineering, Vol. 2*, pp. 537–541.
- Saito, M., 1969. Forecasting time of slope failure by tertiary creep. In: *Proceedings, 7th International Conference on Soil Mechanics and Foundation Engineering, Mexico City*, pp. 677–683.
- Satgada, C.P., Egusa, T., Yamakawa, Y., Imaizumi, F., 2023. Forest harvesting affects soil organic carbon and total nitrogen transports by facilitating landslides. *Catena* 233, 107517. <https://doi.org/10.1016/j.catena.2023.107517>.
- Smethurst, J.A., Smith, A., Uhlemann, S., Wooff, C., Chambers, J., Hughes, P., Lenart, S., Springman, S.M., Lofroth, H., Hughes, D., 2017. Current and future role of instrumentation and monitoring in the performance of transport infrastructure slopes. *Q. J. Eng. Geol. Hydrogeol.* 50, 271–286. <https://doi.org/10.1144/qjegh2016-080>.
- Smith, A.F., 1973. A general Bayesian linear model. *J. R. Stat. Soc. Ser. B* 35 (1), 67–75. <https://doi.org/10.1111/j.2517-6161.1973.tb00937.x>.
- Stähli, M., Sättle, M., Huggel, C., McArdell, B.W., Lehmann, P., Van, H.A., Berne, A., Schleiss, M., Ferrari, A., Kos, A., Or, D., Springman, S.M., 2015. Monitoring and prediction in early warning systems for rapid mass movements. *Nat. Hazards Earth Syst. Sci.* 15 (4), 905–917. <https://doi.org/10.5194/nhess-15-905-2015>.

- Sun, D.L., Xu, J.H., Wen, H.J., 2021. Assessment of landslide susceptibility mapping based on Bayesian hyperparameter optimization: a comparison between logistic regression and random forest. *Eng Geol* 281, 105972. <https://doi.org/10.1016/j.enggeo.2020.105972>.
- Teuku, F.F., Dwikorita, K., Wahyu, W., 2016. An integrated methodology to develop a standard for landslide early warning systems. *Nat. Hazards Earth Syst. Sci.* 16, 2123–2135. <https://doi.org/10.5194/nhess-16-2123-2016>.
- Towhata, I., Uchimura, T., Gallage, C.P.K., 2005. On early detection and warning against rainfall-induced landslide. In: Proc. of the First General Assembly and the Fourth Session of Board of Representatives of the International Consortium on Landslides (ICL). Springer, Washington, DC, pp. 133–139. https://doi.org/10.1007/3-540-28680-2_16.
- Uchimura, T., Towhata, I., Trinh, T.L.A., Fukuda, J., Carlos, J.B.B., Wang, L., Seko, I., Uchida, T., Matsuoka, A., Ito, Y., Onda, Y., Iwagami, S., Kim, M.S., Sakai, N., 2010. Simple monitoring method for precaution of landslides watching tilting and water contents on slopes surface. *Landslides* 7, 351–357. <https://doi.org/10.1007/s10346-009-0178-z>.
- Uchimura, T., Towhata, I., Wang, L., Qiao, J.P., 2011. Miniature ground inclinometer for slope monitoring. In: In: Proceedings of the 14th Asian Regional Conference on Soil Mechanics and Geotechnical Engineering. China, Hong Kong.
- Uchimura, T., Towhata, I., Wang, L., Nishie, S., Yamaguchi, H., Seko, I., Qiao, J., 2015. Precaution and early warning of surface failure of slopes using tilt sensors. *Soils Found.* 55 (5), 1086–1099. <https://doi.org/10.1016/j.sandf.2015.09.010>.
- Voight, B., 1988. A method for prediction of volcanic eruptions. *Nature* 332, 125–130. <https://doi.org/10.1038/332125a0>.
- Walter, G., Augustin, T., 2010. Bayesian linear regression d different conjugate models and their (in) sensitivity to prior-data conflict. In: Kneib, T., Tutz, G. (Eds.), Statistical Modelling and Regression Structures. Physica-Verlag, Heidelberg, Germany, pp. 59–78. https://doi.org/10.1007/978-3-7908-2413-1_4.
- Wang, L., Hwang, J.H., Luo, Z., Juang, C.H., Xiao, J.H., 2013. Probabilistic back analysis of slope failure - a case study in Taiwan. *Comput. Geotech.* 51, 12–23. <https://doi.org/10.1016/j.compgeo.2013.01.008>.
- Wang, Y.K., Huang, J.S., Tang, H.M., Zeng, C., 2020. Bayesian back analysis of landslides considering slip surface uncertainty. *Landslides* 17 (9), 2125–2136. <https://doi.org/10.1007/s10346-020-01432-4>.
- Wang, L., Seko, I., Fukuhara, M., Towhata, I., Uchimura, T., Tao, S., 2022a. Risk evaluation and warning threshold of unstable slope using tilting sensor array. *Nat. Hazards* 114 (1), 127–156. <https://doi.org/10.1007/s11069-022-05383-y>.
- Wang, H.H., Zhong, P., Xiu, D.H., Zhong, Y.S., Peng, D.L., Xu, Q., 2022b. Monitoring tilting angle of the slope surface to predict loess fall landslide: an on-site evidence from Heifangtai loess fall landslide in Gansu Province, China. *Landslides* 19 (3), 719–729. <https://doi.org/10.1007/s10346-021-01727-0>.
- Wasowski, J., Bovenga, F., 2014. Investigating landslides and unstable slopes with satellite multitemporal interferometry: current issues and future perspectives. *Eng. Geol.* 174, 103–138. <https://doi.org/10.1016/j.enggeo.2014.03.003>.
- Wasowski, J., Pisano, L., 2019. Long-term InSAR, borehole inclinometer, and rainfall records provide insight into the mechanism and activity patterns of an extremely slow urbanized landslide. *Landslides* 17, 445–457. <https://doi.org/10.1007/s10346-019-01276-7>.
- Xie, J., Uchimura, T., Chen, P., Liu, J., Xie, C., Shen, Q., 2019. A relationship between displacement and tilting angle of the slope surface in shallow landslides. *Landslides* 16 (6), 1243–1251. <https://doi.org/10.1007/s10346-019-01135-5>.
- Xie, J.R., Uchimura, T., Wang, G.H., Shen, Q., Maqsood, Z., Xie, C.R., Lei, W.K., Tao, S., Chen, P., Dong, H., Mei, G.X., Qiao, S.F., 2020. A new prediction method for the occurrence of landslides based on the time history of tilting of the slope surface. *Landslides* 17, 301–312. <https://doi.org/10.1007/s10346-019-01283-8>.
- Zeng, P., Feng, B., Dai, K., Li, T., Fan, X., Sun, X., 2024. Can satellite InSAR innovate the way of large landslide early warning? *Eng. Geol.* 342, 107771. <https://doi.org/10.1016/j.enggeo.2024.107771>.
- Zhang, J., Wang, Z.P., Zhang, G.D., Xue, Y.D., 2020. Probabilistic prediction of slope failure time. *Eng. Geol.* 271, 105586. <https://doi.org/10.1016/j.enggeo.2020.105586>.
- Zhang, J., Wang, Z.P., Hu, J.Z., Xiao, S.H., Shang, W.Y., 2022. Bayesian machine learning-based method for prediction of slope failure time. *Int. J. Rock Mech. Min. Sci.* 14, 1188–1199. <https://doi.org/10.1016/j.jrmge.2021.09.010>.
- Zhang, J., Xiao, T., Ji, Jian, Zeng, P., Cao, Z.J., 2023. Geotechnical Reliability Analysis. Springer Nature Singapore, Singapore. <https://doi.org/10.1007/978-981-19-6254-7>.
- Zhou, X., Cui, Y., Fang, J., Tang, H., Zhang, Z., Wang, S., 2025. Link between the impact mechanisms of granular flow-dam interaction and the generated seismic signal: Insights from laboratory experiments. *J. Geophys. Res. Solid Earth* 130, e2024JB029946. <https://doi.org/10.1029/2024JB029946>.
- Zhou, X.P., Yuan, X.K., Yang, D., 2024. Prediction of landslide failure time based on moving average convergence and divergence coupling with Bayesian updating method. *Eng. Geol.* 343, 107781. <https://doi.org/10.1016/j.enggeo.2024.107781>.